On-chip, planar integration of Er doped silicon-rich silicon nitride microdisk with SU-8 waveguide with sub-micron gap control

Jee Soo Chang[1], Seok Chan Eom[1], Gun Yong Sung[3] and Jung H. Shin[1,2]

[1]*Department of Physics, KAIST 373-1 Guseong-dong, Yuseong-Gu, Daejeon, Rep. of Korea*
[2]*Graduate School of Nanoscience and Technology (WCU), KAIST*
373-1 Guseong-dong, Yuseong-Gu, Daejeon, Rep. of Korea
[3]*Biosensor Research Team, ETRI, Daejeon 305-700, Rep. of Korea*
jhs@kaist.ac.kr

Abstract: On-chip, planar integration of Er-doped Silicon-rich silicon nitride microdisks with SU-8 waveguide and polymer cladding is achieved. The lack of high temperature or etching processes allows back-end integration without any optical damage to the microcavity resonator. The maximum measured Q-factor at 1475.5 nm was 13,000, corresponding to calculated intrinsic resonator Q-factor of 25,000 that is limited by process-related roughness.

OCIS codes: (230.5750) Resonators; (160.5690) Rare-earth-doped materials.

References and links

1. T. J. Kippenberg, J. Kalkman, A. Polman, and K. J. Vahala, "Demonstration of an erbium-doped microdisk laser on a silicon chip," Phys. Rev. A **74**(5), 051802 (2006).
2. B. Min, T. J. Kippenberg, L. Yang, K. J. Vahala, J. Kalkman, and A. Polman, "Erbium-implanted high-Q silica toroidal microcavity laser on a silicon chip," Phys. Rev. A **70**(3), 033803 (2004).
3. D. S. Gardner, and M. L. Brongersma, "Microring and microdisk optical resonators using silicon nanocrystals and erbium prepared using silicon technology," Opt. Mater. **27**(5), 804–811 (2005).
4. D. H. Hartman, G. R. Lalk, J. W. Howse, and R. R. Krchnavek, "Radiant cured polymer optical waveguides on printed circuit boards for photonic interconnection use," Appl. Opt. **28**(1), 40–47 (1989).
5. R. Dangel, C. Berger, R. Beyeler, L. Dellmann, M. Gmur, R. Hamelin, F. Horst, T. Lamprecht, T. Morf, S. Oggioni, M. Spreafico, and B. J. Offrein, "Polymer-Waveguide-Based Board-Level Optical Interconnect Technology for Datacom Applications," IEEE Trans. Adv. Packag. **31**(4), 759–767 (2008).
6. N. Daldosso, M. Melchiorri, F. Riboli, M. Girardini, G. Pucker, M. Crivellari, P. Bellutti, A. Lui, and L. Pavesi, "Comparison among various Si_3N_4 waveguide geometries grown within a CMOS fabrication pilot line," J. Lightwave Technol. **22**(7), 1734–1740 (2004).
7. J. S. Chang, M.-K. Kim, Y.-H. Lee, J. H. Shin, and G. Y. Sung, "Fabrication and characterization of Er doped silicon-rich silicon nitride(SRSN) micro-disks," Proc. SPIE **6897**, 68970O (2008).
8. I.-K. Hwang, S.-K. Kim, J.-K. Yang, S.-H. Kim, S. H. Lee, and Y.-H. Lee, "Curved-microfiber photon coupling for photonic crystal light emitter," Appl. Phys. Lett. **87**(13), 131107 (2005).
9. W. J. Miniscalco, and R. S. Quimby, "General procedure for the analysis of $Er^{(3+)}$ cross sections," Opt. Lett. **16**(4), 258–260 (1991).
10. D. E. McCumber, "Theory of Phonon-Terminated Optical Masers," Phys. Rev. **134**(2A), A299–A306 (1964).
11. A. Yariv, "Universal relations for coupling of optical power between microresonators and dielectric waveguides," Electron. Lett. **36**(4), 321–322 (2000).
12. L. F. Stokes, M. Chodorow, and H. J. Shaw, "All-single-mode fiber resonator," Opt. Lett. **7**(6), 288–290 (1982).
13. K. J. Vahala, Optical microcavities, Adv. Series in Appl. Phys. (World Scientific, 2004) Vol. 5, Chap. 5.
14. S. Zheng, H. Chen, and A. W. Poon, "Microring-Resonator Cross-Connect Filters in Silicon Nitride: Rib Waveguide Dimensions Dependence," IEEE J. Sel. Top. Quantum Electron. **12**(6), 1380–1387 (2006).
15. D. W. Vernooy, V. S. Ilchenko, H. Mabuchi, E. W. Streed, and H. J. Kimble, "High-Q measurements of fused-silica microspheres in the near infrared," Opt. Lett. **23**(4), 247–249 (1998).
16. F. P. Payne, and J. P. R. Lacey, "A theoretical analysis of scattering loss from planar optical waveguides," Opt. Quantum Electron. **26**(10), 977–986 (1994).
17. M. Borselli, T. J. Johnson, and O. Painter, "Beyond the Rayleigh scattering limit in high-Q silicon microdisks: theory and experiment," Opt. Express **13**(5), 1515–1530 (2005).
18. R. D. Kekatpure, and M. L. Brongersma, "Fundamental photophysics and optical loss processes in Si-nanocrystal-doped microdisk resonators," Phys. Rev. A **78**(2), 023829 (2008).

#118442 - $15.00 USD Received 13 Oct 2009; revised 12 Nov 2009; accepted 20 Nov 2009; published 1 Dec 2009

19. S. Blair, and Y. Chen, "Resonant-enhanced evanescent-wave fluorescence biosensing with cylindrical optical cavities," Appl. Opt. **40**(4), 570–582 (2001).
20. J. H. Shin, M.-Se. Yang, J.-S. Chang, S.-Y. Lee, K. Suh, H. G. Yoo, Y. Fu, and P. Fauchet, "Materials and devices for compact optical amplification in Si photonics," Proc. SPIE **6897**, 68970N (2008).
21. J. S. Chang, I. Y. Kim, K. J. Kim, G. Y. Sung, and J. H. Shin, "Optical loss and gain characterization in Er doped SRSN," to be submitted (2009).

1. Introduction

Trivalent Er ions can amplify light at the technologically important 1.5 μm region through its intra-4f transition from the first-excited to ground state [$^4I_{13/2} \rightarrow {}^4I_{15/2}$], and were the basis for the on-chip, silica micro-resonator lasers for Si photonics that have been reported recently [1, 2]. Unfortunately, the low refractive index of silica precludes fabrication of compact devices with optical cladding necessary for robust operation. Furthermore, since these microdisks must ultimately be integrated with other photonic circuits, most likely on top of an existing electronic circuit, waveguides must be made of a different material without Er in a flexible process. Yet traditional methods of deposition + etching require processing steps that are not only complex, but can also compromise the integrity of pre-existing optical and electrical components.

In this paper, we report on integrating Er-doped silicon-rich silicon nitride (SRSN) microdisk resonators with SU-8 polymer waveguide and polymer cladding. Previous works have indicated the possibility of using SRSN for compact optical devices with controllable, high refractive index and high mode overlap [3], and use of polymer enables easy fabrication of low-loss, Er-free waveguides as well as compatibility with recently reported optical PCB structures [4,5]. We find that this combination of SRSN microdisks and polymer waveguides enables their integration with sub-μm gap control necessary for efficient coupling without any etching or high-temperature processes that can compromise the integrity of existing devices. The maximum measured Q-factor was 13,000 at 1475.5 nm, corresponding to calculated intrinsic resonator Q-factor of 24,800 that is limited by process-related roughness

2. Fabrication and experimental details

Er doped SRSN film with thickness of 490 nm was deposited on a 15 μm thermal oxide substrate by the reactive ion beam sputtering method and subsequently annealing at 950 °C for 30 min. The excess Si and Er contents were 5 and 0.43 at.%, respectively, and refractive index near 1550 nm was 1.991. Photo-lithography and dry etching with amorphous Si hard mask was used to define both the 25-μm diameter microdisks and alignment marks. The etch depth was 680 nm, resulting in over-etching of the nitride layer. SU-8 polymer with refractive index of 1.574 @ 1550 nm was then spin coated, and 2.3 μm wide and 2.2 μm high single-mode channel waveguides were fabricated by UV-curing using photo-litho masks with designed disk-waveguide gap widths. The waveguides were aligned to the existing microdisks using the alignment marks, and additional fine-control over the gap width was also possible by varying UV exposure time. The entire waveguide fabrication and cladding procedure took place at room temperature. Finally, the entire structure was spin coated with ~5 μm thick polymer (FOWG-107) with refractive index of 1.5145, and then cleaved to enable fiber coupling. The propagation loss of SU8 waveguides was measured to be 3.5 dB/cm (data not shown), comparable with other channel-type high index waveguides [6].

3. Measurement and analysis

Figures 1(a)-1(c) show typical scanning electron microscope (SEM) images of fabricated microdisks, integrated with SU8 waveguides. We find that waveguides remain straight and smooth along its entire length. Furthermore, the resonator-waveguide gap is formed without any damage to the existing microdisk resonator, with widths that can be controlled within hundred nm. Figure 1(d) shows the optical microscope image of the sample with 800 nm gap

#118442 - $15.00 USD Received 13 Oct 2009; revised 12 Nov 2009; accepted 20 Nov 2009; published 1 Dec 2009

after polymer cladding. The disk-waveguide gap appears uniform, indicating that polymer cladding successfully infiltrated the gap without forming any macroscopic bubbles.

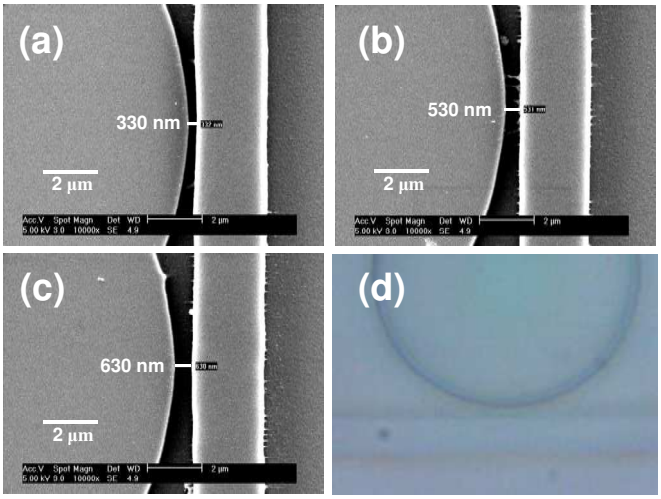

Fig. 1. SEM images of SRSN microdisk integrated with SU 8 waveguide with resonator-waveguide gap of (a) 330, (b) 530, and (c) 630 nm before cladding. (d) Optical microscope image of the microdisk with 800 nm gap after polymer cladding. Note the uniformity of the cladding layer, including the disk-waveguide gap.

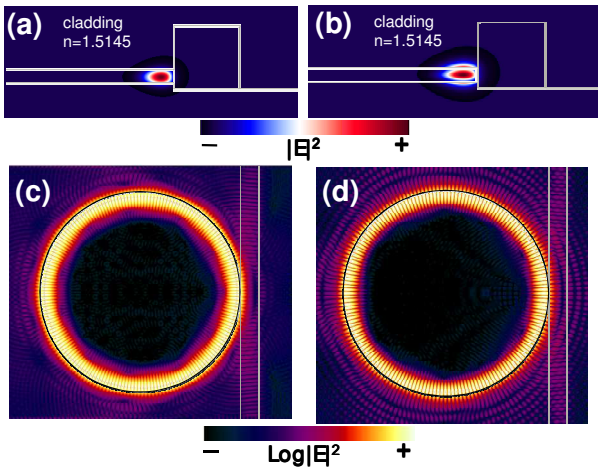

Fig. 2. The calculated $|E|^2$-field distributions of the TE-like and TM-like fundamental modes of the integrated structure, with an azimuthal number of 90 and 86, respectively. The diameter of the disk is 25 μm with a total thickness of 680 nm (SRSN:Er 490 nm/thermal oxide 190 nm). The waveguide is 2.3 μm wide and 2.2 μm high, and is just touching the disk (disk-waveguide gap of 0 nm).

Figure 2 shows the 3D finite-difference time-domain (FDTD) simulation results of the integrated structure with disk-waveguide gap width of 0 nm. The disk and waveguide dimensions obtained from the SEM images were used in simulations, and the mode was excited by a dipole source placed in the disk. As the light is much weaker in the waveguide than in the disk, Figs. 2(c) and 2(d) were drawn in log scale to highlight the coupled light. We find mode overlap values remain high at 0.86 and 0.65 for TE- and TM-like modes, respectively even with polymer cladding. The total Q-factors (coupling loss included) of the integrated structures are estimated from the decay times of excited modes to be 1.57×10^5 for

#118442 - $15.00 USD Received 13 Oct 2009; revised 12 Nov 2009; accepted 20 Nov 2009; published 1 Dec 2009

TE-like mode at the resonance wavelength 1528.9 nm, but only 11,500 for the TM-like mode at 1544.2 nm (data not shown). Thus, we will henceforth concentrate on the TE-like mode only.

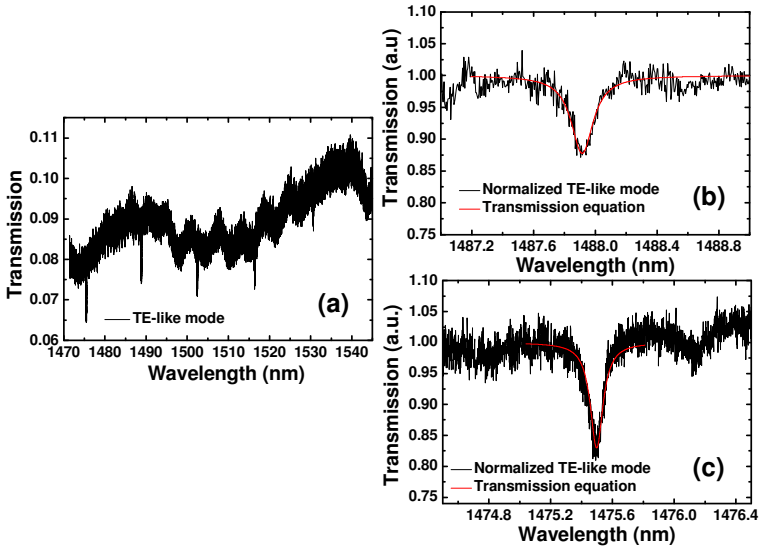

Fig. 3. (a) The transmission spectrum of an integrated microdisk with a resonator-waveguide gap of 800 nm. (c) The transmission dip with the maximum intrinsic Q at wavelength 1475.5 nm in detail. (b) The transmission dip at 1487.8 nm from the same disk, but obtained via tapered fiber coupling method prior to waveguide integration and cladding.

Figure 3(a) shows the transmission spectrum of an integrated microdisk, obtained using TE-polarized input from a continuously tunable, external cavity laser with <300 kHz linewidth that was coupled into, and extracted from the waveguide using a single-mode lensed fiber with radius curvature of 7 ± 2 μm [7]. We observe sharp dips with an FSR of about 15 nm that were verified by FDTD simulation as first-order radial TE-like modes (not shown).

To investigate the effect of integration on the optical qualities of the resonators, the Q-factors of waveguide-integrated microdisk was compared with that obtained from the same disk via tapered-fiber coupling [7,8] prior to waveguide integration. Direct comparison of the measured Q-factors, however, is inappropriate, as they contain the effects of both the coupling loss and the Er absorption loss that can depend on the resonance wavelengths. The Er absorption loss can easily be estimated by $\alpha_{Er} = \sigma N_{Er} \Gamma$, where σ is the Er absorption cross section (taken to be 0.6×10^{-20} cm^2 near 1480 nm [9,10,21]), N_{Er} is the Er concentration, and Γ is the mode overlap, to be 9.2 dB/cm. The coupling loss is calculated by using the universal relation for waveguide coupled microresonators [11,12], given by

$$T = (1-\gamma_o)\left[1 - \frac{\kappa\{1-(1-\gamma_o)e^{-2(\alpha_o+\alpha_{Er})L}\}}{1+(1-\gamma_o)(1-\kappa)\,e^{-2(\alpha_o+\alpha_{Er})L} - 2\sqrt{1-\gamma_o}\sqrt{1-\kappa}\;e^{-(\alpha_o+\alpha_{Er})L}\cos(\beta L)}\right] \quad (1)$$

where γ_o is the loss of the input power, κ is the coupling coefficient. α_o is the propagation loss, and α_{Er} is the Er absorption loss. n and L are the refractive index and circumference of the microdisk, and $\beta = n\omega/c$. The instrinsic Q-factor of the disk, which is independent of coupling or Er-doping, can then be estimated by $1/Q_{tot} = 1/Q_{intrinsic} + 1/Q_{Er} + 1/Q_{coupling}$.

#118442 - $15.00 USD Received 13 Oct 2009; revised 12 Nov 2009; accepted 20 Nov 2009; published 1 Dec 2009

Table 1 The coupling coefficient (κ) and intrinsic cavity Q-factors with and without Er, determined from the transmission spectra by fitting the transmission Eq. (1) [12].

Position	Measured Q (Q_{tot})	κ	Intrinsic Q with Er	$Q_{coupling}$	Intrinsic Q without Er
Waveguide coupled	**(Max)** 12,900 @ 1475.5 nm	0.19 %	15,300 (24 dB/cm)	86,500	24,800 (15 dB/cm)
	(same wavelength) 10,860 @ 1488.9 nm	0.20 %	12,160 (30 dB/cm)	1.0×10^5	17,543 (21 dB/cm)
	(same m = 91) 8,400 @ 1516.4 nm	0.14 %	12,400 (29 dB/cm)	26,000	18,000 (20 dB/cm)
Tapered fiber coupled	**(Max, m = 91)** 10,300 @ 1487.9 nm	0.24 %	11,200 (33 dB/cm)	1.3×10^5	16,076 (23 dB/cm)

Figure 3(b) shows the transmission-dip of microdisk prior to integration with the highest Q-factor, together with the fit to Eq. (1). To this, we compare 3 transmission dips from the integrated structure: one at the same wavelength; one at the same azimuthal number; and the one with the highest Q-factor. Figure 3(c) shows the transmission dip of the integrated microdisk with the highest Q-factor, together with the fit to Eq. (1), and the results of analysis are summarized in Table 1.

We find that $Q_{coupling}$ values are much higher than the intrinsic Q with Er, indicating that we are dealing with, under-coupled conditions in all cases [13]. More importantly, the waveguide-integrated disk has consistently higher Q-values, for both Q_{tot} and $Q_{intrinsic}$, a maximum value of 24,800 for $Q_{intrinsic}$. This value is comparable with the other reported Q factors measured from Er-free nitride based resonators fabricated by photo-lithography [14], and demonstrates that by using polymers, we were able to integrate low-loss waveguide to an existing microresonator without inducing any optical damage. Furthermore, as the entire process takes place at room temperature, we expect that integration would not have damaged any possible electronic circuits as well.

Still, the value of 24,800 is much lower than the radiation-limited $Q_{intrinsic}$, calculated to be $> 10^6$ (data not shown), indicating a large optical loss of 15 dB/cm. Furthermore, $Q_{intrinsic}$ by definition should not depend on integration. To investigate the possible sources of such loss and the reason for improved $Q_{intrinsic}$ after integration, we have first analyzed the surface roughness on the top surface of a microdisk that underwent identical deposition and etching process using the atomic force microscopy (AFM). From Figs. 4(a) and 4(b), the average surface roughness (σ_{rms}) and the lateral correlation length L_c are extracted to be 1.15 ± 0.01 nm and 25 nm [15], respectively. Using these values for the analytical expression for the scattering loss by the surface roughness [16], we calculate that the surface roughness contributes to an optical loss of less than 1 dB/cm. On the other hand, the sidewall roughness on the microdisk induced by lithography and etching processes are much larger, as can be seen in Figs. 4(c) and 4(d). From these SEM images, the edge roughness (σ_{rms}) is estimated to be as large as 10 nm, which, according to Ref [17,18], would lead to scattering loss of about 12 dB/cm. This value is comparable to the intrinsic optical loss of the cavity deduced from the experiments, and indicates that the Q-factor of the fabricated microdisk is limited by the process-related sidewall roughness and not by a fundamental limitation imposed by SRSN, consistent with reports on low-loss devices based on SiN [6]. This is also consistent with observed improvement in $Q_{intrinsic}$, after integration, as polymer cladding would reduce the refractive index contrast at the sidewall, and thereby reduce the scattering losses due to any sidewall roughness. It is also possible, however, that such change in refractive index contrast affects the photon lifetime inside the cavity as well [19].

#118442 - $15.00 USD Received 13 Oct 2009; revised 12 Nov 2009; accepted 20 Nov 2009; published 1 Dec 2009

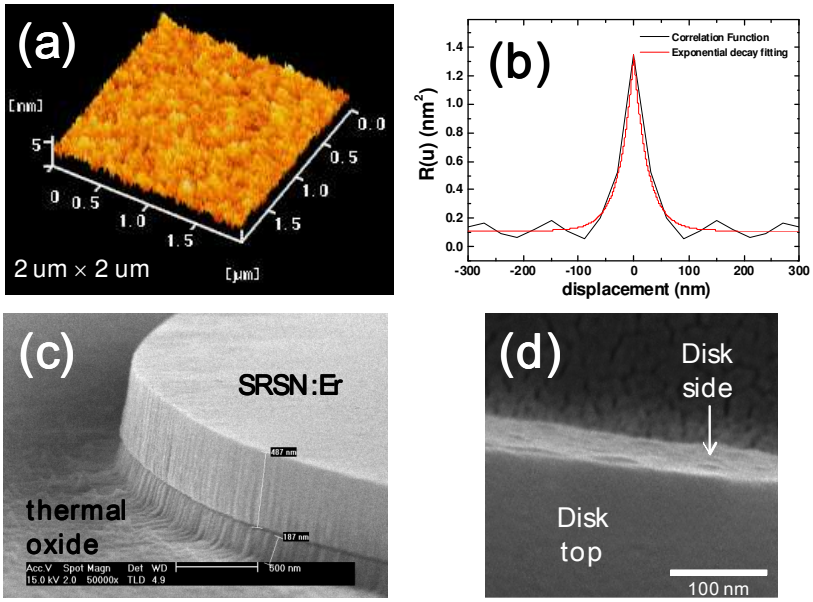

Fig. 4. (a) Top surface roughness data of the fully fabricated microdisk obtained by AFM on a 2 μm square grid. The rms roughness is 1.15 ± 0.01 nm. (b) The correlation function obtained from the AFM data, showing a statistical correlation length of 25 nm. (c), (d) SEM images showing sidewall roughness of microdisks. The rms roughness is as large as 10 nm.

With the integrated structure, robust and stable pumping of the microdisks is possible. As Fig. 5 shows, sharp Er^{3+} emission peaks at resonant wavelengths can easily be obtained from an integrated microdisk when pumped with a 1475 nm laser through the integrated waveguide. However, given the Er concentration and mode overlap, the maximum internal gain that can be obtained from doped Er ions is estimated to be 13 dB/cm only ($\sigma = 0.8 \times 10^{-20}$ cm^2 at 1536 nm). As this value is lower than the intrinsic cavity loss of 15 dB/cm, no net gain and thus no lasing is yet possible. Thus, overcoupling between microdisk and waveguide was required to obtain sufficient signal for Fig. 5.

In fact, as the emission cross-section of Er^{3+} near 1480 nm is non-zero, the maximum population inversion that can be achieved is only ~0.75 [9,10,21], reducing the maximum possible internal gain at 1536 nm to $\sigma N_{Er}\Gamma \times (0.75\text{-}0.25) = 6.5$ dB/cm only. As optical loss of cavity needs to be smaller than the internal gain for lasing to occur, this indicates that minimum $Q_{intrinsic}$ required for lasing is about 60,000. We note, however, that several factors such as optical de-activation of doped Er, non-linear effects such as cooperative up-conversion, and waveguide coupling loss will increase the minimum required Q-factor for lasing. Still, we have previously reported that optical de-activation of Er in nitrides is significantly suppressed compared to that in oxides [20,21]. Furthermore, by employing undercoupled waveguides, the coupling loss can be controlled as well. Thus, a more reasonable estimate of three-fold improvement of $Q_{intrinsic}$ to 75,000 would be needed for development of efficient, fully integrated microdisk laser on a Si chip.

4. Conclusion

In conclusion, we have demonstrated the fabrication of Er-doped silicon-rich silicon nitride planar type microdisks integrated in an all-planar fashion with a SU-8 polymer waveguide and cladding on a single chip. Use of polymer enables gap control and integration at room temperature without complex deposition + etching processes that can damage the pre-existing optical and/or electrical devices, and use of silicon-rich silicon nitride enables compact optical

#118442 - $15.00 USD Received 13 Oct 2009; revised 12 Nov 2009; accepted 20 Nov 2009; published 1 Dec 2009

devices with high mode overlap for efficient Er pumping. The maximum measured Q-factor at 1475.5 nm was 13,000, corresponding to calculated intrinsic resonator Q-factor of 24,800 that is limited by process-related roughness. We expect that with a three-fold reduction in optical losses by improving fabrication process, a fully integrated microdisk laser on a chip would be possible.

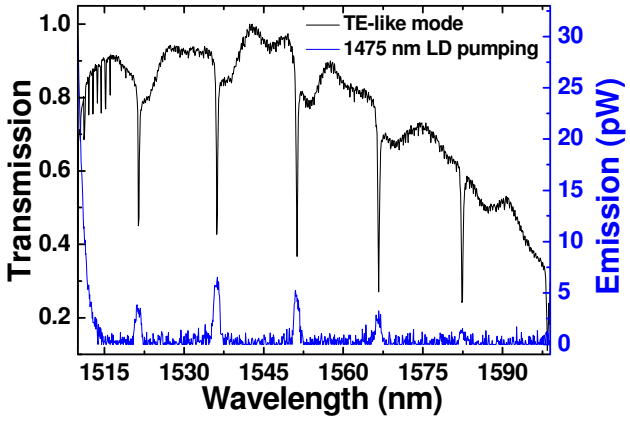

Fig. 5. Transmission spectrum of an over-coupled integrated structure showing the resonance dips, and corresponding Er^{3+} emission peaks at the same wavelength obtained by pumping the microdisk with a 1475 nm laser diode via the integrated waveguide. The widths of emission peaks are limited by OSA resolution, set at 1.0 nm.

Acknowledgement

This work was supported in part by grant No. R01-2007-000-21036-0, by OPERA of the Korea Science and Engineering Foundation (KOSEF), by WCU (World Class University, grant No.R31-2008-000-10071-0) program through the KOSEF and Engineering Foundation funded by the Ministry of Education, Science and Technology (MEST). This work was partly supported by the Top Brand R&D program of MKE (09ZC1410: Basic Research for the Ubiquitous Lifecare Module Development) in Korea.

#118442 - $15.00 USD Received 13 Oct 2009; revised 12 Nov 2009; accepted 20 Nov 2009; published 1 Dec 2009